

Measurement of Femtosecond Ionization Dynamics of Atmospheric Density Gases by Spectral Blueshifting

Wm. M. Wood, C. W. Siders, and M. C. Downer

Physics Department, University of Texas at Austin, Austin, Texas 78712

(Received 5 August 1991)

The new plasma diagnostic technique of spectral blueshifting of femtosecond pulses is used for the first time to analyze quantitatively the ionization of noble gases under the influence of intense, femtosecond illumination. The two processes of strong-field tunneling ionization and electron impact ionization are found to play competing roles on these time scales.

PACS numbers: 52.40.Nk, 32.80.-t, 34.80.Dp, 52.25.Jm

Highly ionized plasmas approaching atmospheric density are a potential future source of coherent x rays [1], and a potential medium for charged-particle acceleration [2]. Ionization by intense, femtosecond pulses holds promise for precise control of initial plasma conditions (temperature, ionization state, density) [3] which are critical to these applications. At the same time, new, quantitative, experimental diagnostics compatible with the high gas density and ultrafast time scale are needed to measure the ionization and subsequent plasma dynamics which give rise to these conditions. A number of authors have shown, both experimentally and theoretically, that a laser pulse which rapidly ionizes a gas experiences a frequency blueshift caused by the creation of a free-electron plasma [4,5]:

$$\Delta\omega = -\frac{\omega_0}{c} \int_0^z \frac{\partial n}{\partial t}(l) dl. \quad (1)$$

Here, ω_0 is the angular frequency of the light, l is the longitudinal distance over which the interaction occurs; $n = (1 - \omega_p^2/\omega_0^2)^{1/2}$ is the index of refraction of the medium through which the pulse travels, and is found using the Drude model (ω_p is the plasma frequency.) In experiments which used pulse durations long with respect to ion-ion collision times [4], plasma expansion and recombination following the ionization contributed to and complicated the phase modulation induced on the pulse. In a previous publication [6], we showed for the first time that *femtosecond* pulses, tightly focused to intensities above the ionization threshold, experience a "pure" blueshift, i.e., with no trace of components redshifted from the original pulse spectrum, indicating qualitatively that the phase modulation on the laser pulse is caused entirely by ionization. Furthermore, complicating nonlinear optical interactions with neutral gas, which can induce spectral *broadening* (supercontinuum) and self-focusing on femtosecond pulses focused more loosely (below the ionization threshold) in dense ($p > 40$ atm) gases [7], were suppressed at near atmospheric pressures because of the lower density and rapid plasma growth early in the tightly focused pulse [6]. This preliminary result suggested that femtosecond time-resolved measurement and analysis of the spectral shifts could measure detailed growth dynamics of the ionization front over a broad range of gas pressures and gas species, distinct from the subsequent

plasma dynamics and optical nonlinearities of the neutral gas. In a wider context, such frequency upshifts might also quantitatively diagnose plasma density oscillations in plasma-based particle accelerator schemes [8].

The purpose of this Letter is to demonstrate, for the first time, the quantitative use of this plasma diagnostic technique in analyzing the breakdown of noble gases caused by intense, femtosecond illumination. This will be done in three stages: (1) We report systematic observations of the self-blueshifting of laser pulses after ionizing 1–5-atm pressure samples of He, Ne, Ar, Kr, and Xe, which reveal a universal, reproducible pattern in the shape of the blueshifted spectra. Specifically, with increasing laser intensity, gas pressure, and atomic number, the self-blueshifted spectra develop from a near replica of the incident pulse spectrum into a complex structure consisting of two spectral peaks: a narrow peak shifted between 5 and 10 nm towards the blue from the original spectrum, and a broad peak shifted further towards the blue whose position and width depend strongly on the gas pressure, gas species, and the laser-pulse energy. (2) We report time-resolved spectral shifts of a weak probing pulse which show different temporal evolution for each of these two spectral features. (3) Finally, we propose a quantitative, *ab initio* model which relates these two spectral features to two competing ionization mechanisms: collisionless tunneling ionization, predicted to dominate early in the ionizing pulse profile, and electron-impact ionization, predicted to dominate in the maximum of the pulse profile.

In our experiments, 100-fs laser pulses with center wavelength of 620 nm and energies up to 0.4 mJ are focused at $f/5$ to a peak intensity of $10^{16 \pm 0.3}$ W/cm² into a glass cell containing 1–5 atm of He, Ne, Ar, Kr, or Xe. All of the light transmitted through the focal region is collected and analyzed by a spectrometer. Typically, less than 1% of the pulse energy is lost in ionizing the gas. Autocorrelation measurements [6(b)] after the interaction region show only $\sim 10\%$ temporal broadening. Figure 1(a) shows the measured spectrum of the ionizing pulse after breakdown in 5 atm Kr. As pulse energy increases, the spectrum blueshifts with little change in shape until the pulse energy reaches 0.1 mJ [$\log_{10}(\text{intensity}) = 15.0$], after which the position of the peak changes very little. As the energy increases further, a shoulder

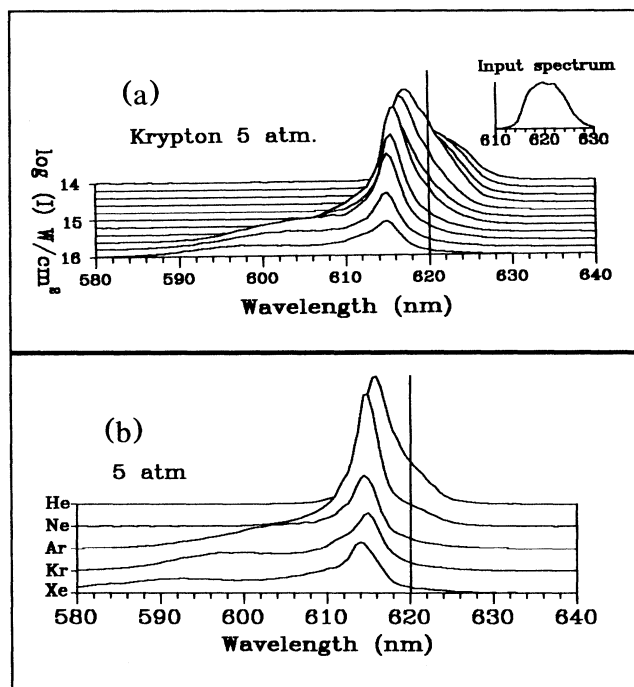


FIG. 1. (a) Spectra after interaction with 5-atm pressure Kr as a function of pulse energy. Pulse energy is increasing towards the bottom in steps of $\times 10^{0.2}$. (b) Spectra after interaction of 0.25-mJ pulses in 5-atm pressure of each of the noble gases studied.

appears on the blue side of the spectrum, then broadens and shifts further towards the blue. Figure 1(b) shows self-shifted spectra after ionization of 5 atm of each of the noble gases using 0.25-mJ pulses. The center of the unshifted pulse spectrum is indicated by a vertical line, showing that a blueshift occurs in all cases. However, the shape of the blueshifted spectrum depends strongly on gas species. In Ar, Kr, and Xe, the narrow, less-shifted peak and the broad, blue shoulder are clearly discernible, the latter becoming a separate peak in Kr and Xe. In He and Ne, the blue shoulder is absent, and a different feature—a “red shoulder” corresponding approximately to the unshifted spectrum—appears showing that some of the initial pulse energy remains unshifted. Although the amplitude and width of each of these spectral features depend on the focal profile, chirp, and other details of the ionizing pulse, numerous measurements have confirmed that the qualitative trends shown in Fig. 1 and described above are universal, reproducible features of femtosecond ionization of the noble gases. Modest defocusing of the transmitted pulse and a visible breakdown “spark” (i.e., recombination luminescence) always accompany, and are precisely correlated with, the onset of the blueshift, consistent with their common origin in the rapid formation of a reduced index plasma [6].

Time-resolved pump-probe experiments show that each of these spectral features also has a characteristic temporal evolution within the pump pulse. To obtain time-

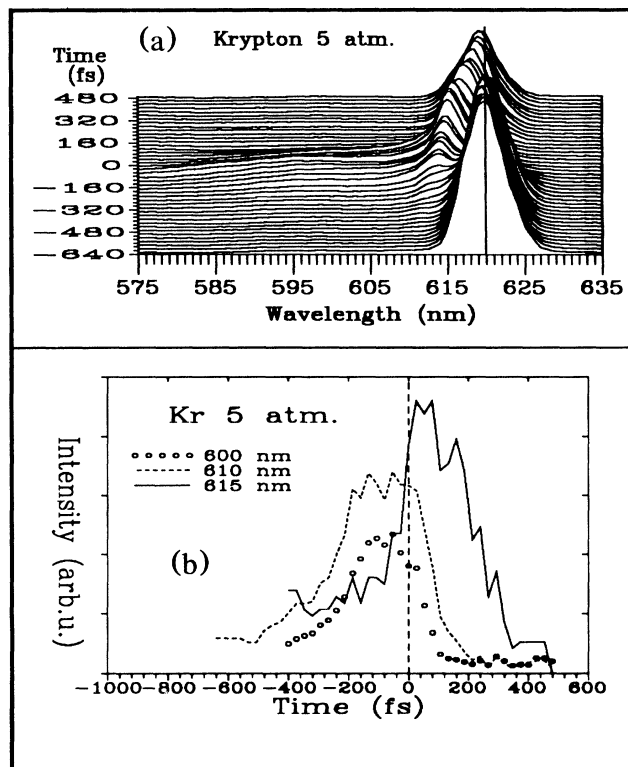


FIG. 2. (a) Time-resolved spectra in krypton at 5 atm using pump pulse energy of 0.22 mJ. There are 27 fs between spectra; time increases towards the top of the figure, with negative times corresponding to the probe pulse arriving before the pump pulse. Coincidence of the pump and probe pulses is indicated by an emboldened spectrum. (b) Energies at 600, 610, and 615 nm as functions of time for time-resolved spectra in 5 atm Kr.

resolved blueshifted spectra a weak probe pulse, derived from the pump with a beamsplitter, was polarized orthogonally to the ionizing pulse, then copropagated through the focal region before ($\Delta t < 0$), coincident with, or after ($\Delta t > 0$) the pump pulse. The probe was separated from the pump after the interaction region by a polarization analyzer, and its spectrum recorded for different Δt . Figure 2(a) shows a series of time-resolved probe spectra resulting from ionization of 5 atm Kr by a pump pulse centered at $\Delta t = 0$. Coincidence was determined to within ± 20 fs by slightly turning the pump polarization, and then adjusting an optical delay line to maximize the contrast of the resulting pump-probe interference fringes. The probe spectra around $\Delta t = 0$ exhibit the same dual structure seen in the self-shifted spectrum [Fig. 1(a)]. However, close examination shows that the less-shifted peak and the broad bluer shoulder evolve differently in time. To show this contrast quantitatively, we have plotted in Fig. 2(b) the area under the spectra in small regions around 615, 610, and 600 nm. The values at 610 and 600 nm display the same temporal behavior, with maxima at approximately 100 fs before the maximum of the ionizing pulse, indicating that the process giving rise

to the blue shoulder occurs in the early part of the pulse. The values plotted for 615 nm show a maximum approximately 50 fs after the maximum of the pump pulse, indicating that the process causing the narrow, less-shifted peak occurs near or slightly after the maximum of the ionizing pulse. A similar time development is observed for the two corresponding blueshifted features for Kr and Ar. The single blueshifted peak for He and Ne, on the other hand, evolves early in the pump profile, with little or no probe blueshift observed for $\Delta t > 0$. Again, quantitative details of the temporal evolution depend on focal profile, but the qualitative trends are observed reproducibly [9].

We now propose a simple, *ab initio* ionization model which accounts for (1) the two blueshifted features observed in Ar, Kr, and Xe, (2) their respective temporal behavior, and (3) the “unshifted” portions of the spectra and the *absence* of the blue shoulder observed in He and Ne. In the presence of a strong light field, the ionization of the atoms can be modeled using the strong-field tunneling theory due to Keldysh or Ammosov, Delone, and Krainov [10], which yield similar results for the lower stages of ionization. The coupled equations governing the densities N_i of atoms of a particular ionization state i are written in the following way:

$$\frac{dN_i}{dt} = (P_{i-1}N_{i-1} - P_iN_i) + (N_e\sigma_{i-1}v_eN_{i-1} - N_e\sigma_i v_e N_i). \quad (2)$$

The first parenthetical term on the right describes the rate of growth of the i th ionization stage, where P_k is the probability per unit time [10] for electrons to tunnel from k -times ionized parent ions. The second term describes collisional ionization via electron impact, where N_e is the free-electron density, v_e is the rms electron velocity, and σ is the cross section [11] for the process. Intermediate resonant states can be ignored under our conditions [12]. The density $N_e(t)$ of free electrons and the resulting index of refraction $n(t)$ calculated from Eq. (2) yields a calculated blueshift upon substitution into Eq. (1). The model using only the tunneling ionization terms P_k adequately describes the observed blueshifting in He and Ne. Because tunneling ionization occurs almost entirely during the first half of the laser pulse, only the leading edge of the pulse becomes blueshifted; the trailing part of the pulse remains unshifted, and appears as the spectral “red” shoulder observed in the He and Ne gas breakdown.

At Ar, Kr, and Xe pressures > 1 atm and with maximum pump intensity, the red unshifted shoulder disappears, and the *entire* pulse spectrum is shifted [Fig. 1(b)]. This observation implies that ionization occurs during and after the peak of the ionizing pulse, and can be explained by including electron-impact ionization [the second parenthetical term of Eq. (2)]. Collisional ionization is strongest near the peak of the laser pulse because (1) the cross sections are maximal for electron energies in

the range 100–500 eV [11], very close to the electron quiver energy at the peak (370 eV for 10^{16} W/cm²); (2) N_e is large due to the strong-field ionization early in the pulse; and (3) the rms velocity v of free electrons is maximal at the peak of the pulse. Stated from a different viewpoint, for the first few charge states, the thresholds for semiclassical barrier suppression ionization (BSI) [13] are less than those for collisional ionization (defined as the intensity at which the quiver energy equals the low-field ionization energy), while for subsequent ionization stages the collisional threshold is reached before the barrier suppression threshold [13]. Estimates of typical ionizing collision times in both He and Ne, where observations imply little or no collisional effect, yield τ

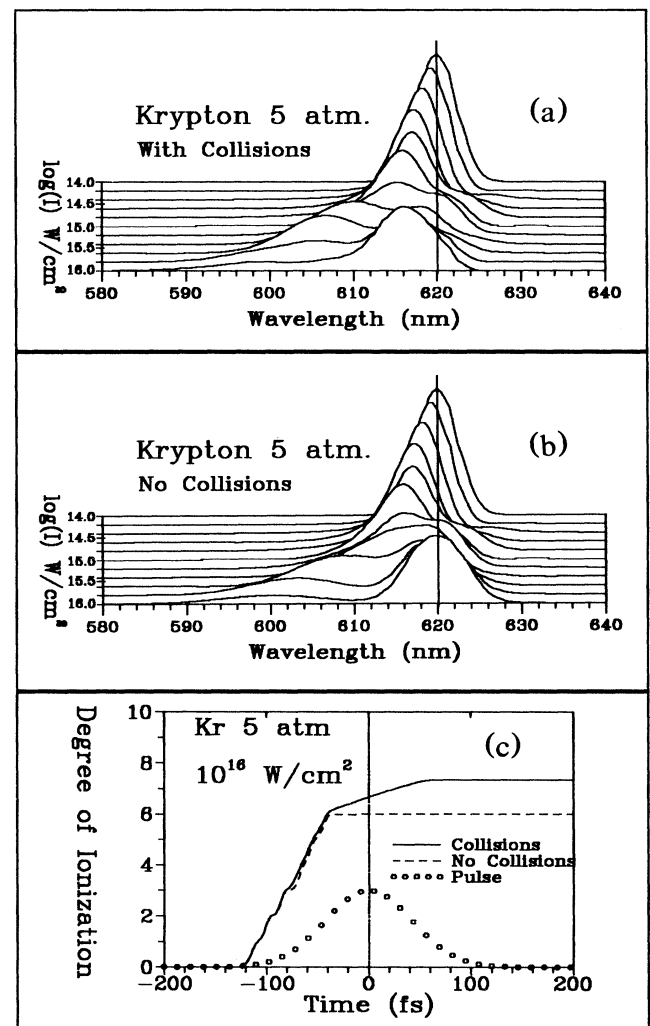


FIG. 3. (a) Calculated self-shifted spectra for ionization of 5 atm Kr by 100-fs pulses of varying peak intensities, using Ammosov strong-field and collisional ionization terms. (b) Calculated spectra for ionization of 5 atm Kr without collisions in the model. (c) Degree of ionization vs time calculated both with and without collisions in 5-atm Kr gas peak intensity of 10^{16} W/cm².

$\sim (N_e \sigma v)^{-1} \sim 200$ fs, significantly *longer* than the light pulse duration. In Ar, Kr, and Xe at 5-atm pressure, however, these collision times are significantly *shorter* than the pulse duration ($\tau < 30$ fs), resulting in significant ionization near the peak of the pulse, and a shifting of the *entire* pulse spectrum.

Figure 3(a) shows the calculated spectra after breakdown of 5 atm Kr, for peak intensities ranging from 10^{14} to 10^{16} W/cm², calculated using Eq. (2) with collisions and a simplified cylindrical interaction region with constant transverse intensity [14]. Figure 3(b) shows the spectra calculated *without* collision ionization: Significant unshifted energy remains in these spectra as peak intensity increases [Fig. 3(b)]. *With* collisions in the model, the *entire* pulse spectrum is shifted, following the same trend as observed in the data. The broad, blue shoulder observed in the data for Ar, Kr, and Xe corresponds to strong-field ionization (and thus has the same origin as the blueshifts observed in He and Ne), while the narrow, less-shifted peak corresponds to slower collisional impact ionization. The calculated temporal behavior of the two features further corroborates this interpretation. Figure 3(c) shows the calculated degree of ionization as a function of time in 5 atm Kr illuminated by a 100-fs pulse with a peak intensity of 10^{16} W/cm², both with and without collisions. Collisional ionization, like the smaller blueshift which it causes, occurs during and after the peak of the pulse, and is slower than strong-field ionization, which causes the larger blueshift early in the pulse. This temporal behavior is also observed in Xe at lower pressures, and in 5 atm Ar. Because of the tight focus and the early onset of ionization in the pulse profile, the calculated blueshift is negligibly affected by including self-phase modulation caused by n_2 of the neutral gas, ions, and electrons, as shown in detail elsewhere [6(b), 15].

In conclusion, the model predicts a high rate of ionization early in the laser pulse due to collisionless strong-field ionization, followed by collisional ionization at a lower rate near the peak of the laser pulse, in good agreement with the data. A more detailed report of the experiments and model will be published separately [16].

This research was supported by the National Science Foundation (Grant No. DMR8858388), the Robert A. Welch Foundation (Grant No. F-1038), and the Air Force Office of Scientific Research (Contract No. F49620-89-C-0044).

- [1] W. W. Jones and A. W. Ali, J. Appl. Phys. **48**, 3118 (1977); J. Peyraud and N. Peyraud, J. Appl. Phys. **43**, 2993 (1972).
- [2] T. Tajima and J. M. Dawson, Phys. Rev. Lett. **43**, 297 (1979); P. Sprangle *et al.*, Appl. Phys. Lett. **53**, 2146 (1988).
- [3] N. H. Burnett and P. B. Corkum, J. Opt. Soc. Am. B **6**, 1195 (1989); B. Penetrante and J. N. Bardsley, Phys. Rev. A **43**, 3100 (1991).

- [4] E. Yablonovitch, Phys. Rev. A **10**, 1888 (1974).
- [5] S. C. Wilks, J. M. Dawson, and W. B. Mori, Phys. Rev. Lett. **61**, 337 (1988).
- [6] (a) Wm. M. Wood, G. B. Focht, and M. C. Downer, Opt. Lett. **13**, 984 (1988); (b) M. C. Downer *et al.*, in *Proceedings of the Tenth International Conference on Spectral Line Shapes*, edited by L. Frommhold and J. W. Keto, AIP Conf. Proc. No. 216 (AIP, New York, 1990).
- [7] P. B. Corkum, C. Rolland, and T. Srinivasan-Rao, Phys. Rev. Lett. **57**, 2268 (1986); J. H. Glowina *et al.*, J. Opt. Soc. Am. B **3**, 1573 (1986); H. J. Lehmeier, W. Leupacher, and A. Penzkofer, Opt. Commun. **56**, 67 (1985).
- [8] E. Esarey, A. Ting, and P. Sprangle, Phys. Rev. A **42**, 3526 (1990); S. C. Wilks *et al.*, Phys. Rev. Lett. **62**, 2600 (1989).
- [9] Note that the nonlinear index $n_2 > 0$ of the neutral gases or ions, if significantly present, would induce a rising index (redshift) in the leading edge of the pulse and a falling index (blueshift) in the trailing edge, contrary to the observed blueshift in the leading edge, which must therefore be caused solely by ionization.
- [10] L. V. Keldysh, Zh. Eksp. Teor. Fiz. **48**, 874 (1965) [Sov. Phys. JETP **21**, 1307 (1965)]; M. V. Ammosov, N. B. Delone, and V. P. Krainov, Zh. Eksp. Teor. Fiz. **91**, 2008 (1986) [Sov. Phys. JETP **64**, 1191 (1986)].
- [11] H. Tawara and T. Kato, At. Data Nucl. Data Tables **36**, 167-353 (1987). Impact-ionization cross sections for intensely irradiated atoms and ions are probably larger than the values for ground-state atoms and ions given in these tables and used in our calculations.
- [12] P. B. Corkum, N. H. Burnett, and F. Brunel, Phys. Rev. Lett. **62**, 1259 (1989).
- [13] S. Augst, D. D. Meyerhofer, D. Strickland, and S. L. Chin, J. Opt. Soc. Am. B **8**, 858 (1991). For example, using the BSI model, we obtain the following threshold intensities for the first seven ionization stages in Kr: $\log_{10}(I_{BSI}) = 14.19, 14.54, 14.92, 15.28, 15.45, 15.56, 16.09$ W/cm², $\log_{10}(I_{coll}) = 14.59, 14.83, 15.01, 15.16, 15.26, 15.32, 15.49$ W/cm².
- [14] Calculations which include convolution over realistic transverse intensity profiles have also been done and yield the same qualitative spectral features as shown in Figs. 3(a) and 3(b), typically with peaks of somewhat different widths and amplitudes. Since, however, the geometry of the interaction region is not quantitatively characterized because of defocusing, calculations using the simpler geometry are presented to illustrate the essential physics.
- [15] The ionization-induced index change $\Delta n_{\text{plasma}} \cong -2\pi n_e^2/m \sim -0.02$ for 1-atm triply ionized plasma exceeds even the hypothetical nonlinear index $n_2^{\text{neutral}} I$ which would be induced by light of intensity $I = 10^{16}$ W/cm² interacting with neutral He, Ne, Kr, and Ar (for Xe, $n_2^{\text{neutral}} I \cong \Delta n_{\text{plasma}}$), using measured n_2^{neutral} values (Lehmeier *et al.*, Ref. [7]). Taking into account the disappearance of the neutral gas early in the pulse, and the smaller n_2^{ion} values of the ions, $n_2^{\text{ion}} I$ is small compared to Δn_{plasma} at the peak of our pulse in all the noble gases. As for the free electrons, n_2^{electron} becomes significant only for relativistic quiver velocities ($I \sim 10^{18}$ W/cm²).
- [16] Wm. M. Wood, C. W. Siders, and M. C. Downer (to be published); Wm. M. Wood, Ph.D. dissertation, University of Texas at Austin, 1991 (unpublished).